

# Thermodynamic View of Activation Energies of Proton Transfer in Various Gramicidin A Channels

Anatoly Chernyshev and Samuel Cukierman

Department of Physiology, Loyola University Medical Center, Maywood, Illinois 60153 USA

**ABSTRACT** The temperature dependencies (range: 5–45°C) of single-channel proton conductances ( $g_H$ ) in native gramicidin A (gA) and in two diastereoisomers (SS and RR) of the dioxolane-linked gA channels were measured in glycerylmonooleate/decane (GMO) and diphytanoylphosphatidylcholine/decane (DiPhPC) bilayers. Linear Arrhenius plots ( $\ln(g_H)$  versus  $K^{-1}$ ) were obtained for the native gA and RR channels in both types of bilayers, and for the SS channel in GMO bilayers only. The Arrhenius plot for proton transfer in the SS channel in DiPhPC bilayers had a break in linearity around 20°C. This break seems to occur only when protons are the permeating cations in the SS channel. The activation energies ( $E_a$ ) for proton transfer in various gA channels (~15 kJ/mol) are consistent with the rate-limiting step being in the channel and/or at the membrane-channel/solution interface, and not in bulk solution.  $E_a$  values for proton transfer in gA channels are considerably smaller than for the permeation of nonproton currents in gA as well as in various other ion channels. The  $E_a$  values for proton transfer in native gA channels are nearly the same in both GMO and DiPhPC bilayers. In contrast, for the dioxolane linked gA dimers,  $E_a$  values were strongly modulated by the lipid environment. The Gibbs activation free energies ( $\Delta G_o^\#$ ) for protons in various gA channels are within the range of 27–29 kJ/mol in GMO bilayers and of 20–22 kJ/mol in DiPhPC bilayers. The largest difference between  $\Delta G_o^\#$  for proton currents occurs between native gA (or SS channels) and the RR channel. In general, the activation entropy ( $\Delta S_o^\#$ ) is mostly responsible for the differences between  $g_H$  values in various gA channels, and also in distinct bilayers. However, significant differences between the activation enthalpies ( $\Delta H_o^\#$ ) for proton transfer in the SS and RR channels occur in distinct membranes.

## INTRODUCTION

Gramicidin A (gA) is a pentadecapeptide whose primary structure consists mostly of an alternating sequence of D- and L-amino acids. The association via six intermolecular H-bonds between the amino termini of two gA molecules in the plane of a lipid bilayer causes the formation of an ion channel that is selective to monovalent cations (Hladky and Haydon, 1972; Koeppe and Andersen, 1996; Urry, 1971). Disruption of those intermolecular H-bonds results in the dissociation of gA monomers with the loss of channel activity. Two gA molecules have been covalently linked with various chemical groups (Bamberg and Janko, 1977; Cukierman et al., 1997; Rudnev et al., 1981; Stankovic et al., 1989; Urry, 1971). In lipid bilayers, these proteins also formed ion channels whose average lifetimes in the open state were considerably longer than native gA channels. Such observations are consistent with the notion that ion channels formed by native gA molecules have a dimeric structure in lipid bilayers. One important advantage of studying single channels of covalently linked gA dimers is that the linkers can be modified by changing or adding simple chemical groups, and the functional consequences of those modifications can be investigated at both the experimental and theoretical levels (Stankovic et al., 1990; Arm-

strong et al., 2001). The relative simplicity of synthetic covalently linked gA dimers provides an interesting and important tool to inquire into the nature of structure-function relationships in ion channels.

In our laboratory, gAs have been covalently linked with a dioxolane group (Cukierman et al., 1997; Quigley et al., 1999). Because of the presence of two chiral carbons in the dioxolane linker, the SS or the RR versions of dioxolane-linked gramicidin A channel can be synthesized (Stankovic et al., 1989). It has been demonstrated that both the SS and the RR dioxolane-linked gA dimers form ion channels in lipid bilayers. Most interestingly, however, is the fact that their channel properties differ in several meaningful and insightful ways (Armstrong et al., 2001; Cukierman et al., 1997; Cukierman, 1999, 2000; Godoy and Cukierman, 2001; Quigley et al., 1999, 2000; Stankovic et al., 1989). In particular, our laboratory has been focusing on studies of the single-channel conductance to protons ( $g_H$ ) in the SS and RR dioxolane-linked gA dimers. The major experimental differences between these diastereoisomers are: 1)  $g_H$  is 2–4-fold larger in the SS than in the RR dimer; 2) although in the SS there is a linear relationship between  $\log(g_H)$  and  $\log([H])$ , such relationship for the RR is more complex and seems to be consistent with proton binding to the channel; and 3) although the open state of the SS channel is stable in lipid bilayers made of either glycerylmonooleate/decane (GMO) or a mixture of phosphatidylethanolamine (PE) and phosphatidylcholine (PC), the open state of the RR channel is not. The RR channel inactivates within a few minutes after forming a channel in the lipid bilayer (GMO or PEPC in decane). Such inactivation, however, does not occur

Received for publication 3 July 2001 and in final form 21 September 2001.

Address reprint requests to Dr. Samuel Cukierman, Department of Physiology, Loyola University Medical Center, 2160 South First Avenue, Maywood, IL 60153. Tel.: 708-216-9471; Fax: 708-216-6308; E-mail: scukier@lumc.edu.

© 2002 by the Biophysical Society

0006-3495/02/01/182/11 \$2.00

when the channel is studied under conditions in which alkaline metals are the conducting cations (Armstrong et al., 2001).

The analysis of the temperature dependence of single-channel conductances always provides essential information on the physicochemical characteristics of ionic permeation inside channels (Akeson and Deamer, 1991; DeCoursey and Cherny, 1998; Jordan, 1999; Miller 1988). Our goal in this study was to further our understanding of proton transfer in the SS and in the RR dioxolane-linked gA dimers by determining the activation energies of  $g_H$  in the temperature range of 5–45°C. To evaluate the energetic consequence of inserting a SS or RR dioxolane linker between two gA molecules, the temperature dependence of  $g_H$  in native gA channels was also examined under the same experimental conditions. Because  $g_H$  in the dioxolane-linked or native gA channels is significantly modulated by the lipid composition of the bilayer (Cukierman et al., 1997; Godoy and Cukierman, 2001; Quigley et al., 1999; Phillips et al., 1999), the temperature effects on  $g_H$  were measured in gA channels reconstituted in either glycerylmonooleate (GMO) or in diphtanoylphosphatidylcholine (DiPhPC) bilayers.

## MATERIALS AND METHODS

### Bilayer set-up

Planar lipid bilayers were formed from a decane solution (60 mg/ml) of either GMO (NuCheck Co., Elysian, MN) or DiPhPC (Avanti Lipids, Alabaster, AL). Planar bilayers were formed on a 100- $\mu$ m-diameter hole separating two aqueous compartments. The thinning of the bilayer was monitored by eye inspection and/or by capacitance measurements. The bilayer chamber was nested inside a hollow aluminum block. The temperature during the experiments was set and controlled by circulating water at the appropriate temperature (Isotemp Circulator 3016, Fisher Scientific, Chicago, IL) inside the metal block. The temperature was constantly monitored throughout the experiments within an accuracy of 0.1°C by a small thermistor probe (YSI 427, Yellow Springs Instruments, Yellow Springs, OH) immersed in the bilayer chamber.

### gA channels

The synthesis, purification, and characterization of dioxolane-linked gA channels were previously described (Quigley et al., 1999; Stankovic et al., 1989). The native gA channels used in this study were purchased from Fluka (Milwaukee, WI). gA channels were added from a methanol stock solution ( $\sim 10^{-8}$  M) that was routinely stored at  $\sim -15^\circ\text{C}$ .

### Single-channel current measurements

Single ion channel currents were measured by voltage clamping the lipid bilayer using an Axopatch 200B (Axon Instruments, Union City, CA). For native gA channels, constant DC voltage steps (to 50 or 100 mV) were applied across the membrane. For the covalently linked gA dimers, voltage clamp ramps from 0 to  $\sim 100$  mV were applied in  $\sim 5$  s. Clampex 8.1 software (Axon Instruments) was used for applying voltages and recording single-channel currents. Within this voltage range and using 1 M HCl solutions, current-voltage relationships for proton currents in the SS or RR channels are ohmic. For each temperature, at least five distinct single-

channel measurements were obtained from at least two distinct lipid bilayers. Most experiments in this study consisted in measuring proton currents in 1 M HCl bulk solution. In other experiments, single-channel conductances to  $\text{K}^+$  ( $g_K$ ) were measured in a 1 M KCl solution. Experimental points in this study are shown as mean  $\pm$  SEM. In most plots, the error bars of the experimental points are smaller than the size of the symbols. Ratios between the standard deviation and the mean of a given set of measurements ( $g_H$  at a given temperature) were typically in the 2–8% range.

## Analysis

Experimental results were analyzed using Sigmaplot 6.0 (SPSS, Chicago, IL). The single-channel conductances for the SS and RR channels in this study were measured from the linear portion of  $I$ - $V$  plots (usually between the voltages of 0 and  $\sim 75$  mV). Single-channel conductances for native gA channels were measured at 50 or 100 mV. The experimental points were plotted as  $\ln(g_H)$  versus  $1/T$  (Arrhenius plots), and the linear relationships were calculated according to

$$g_H = Q \exp\left(\frac{-E_a}{RT}\right), \quad (1)$$

where  $Q$  is the preexponential factor (see below),  $E_a$  is the activation energy, and  $R$  and  $T$  are the gas constant and absolute temperature, respectively.

It can be shown (Guerasimov et al., 1974; Berry et al., 2000) that a thermodynamically related Eyring rate equation for the activated complex state can be written as

$$k_H = \chi \frac{kT}{h} \exp\left(\frac{\Delta S_o^\ddagger}{R}\right) \exp\left(\frac{-\Delta H_o^\ddagger}{RT}\right) \exp\left(\frac{zF\Delta V}{RT}\right), \quad (2)$$

where  $k_H$  is the rate constant for proton transfer in a given gA channel (see below),  $\chi$  is the transmission coefficient (assumed to be 1),  $k$  and  $h$  are the Boltzmann and Planck's constants, respectively,  $z$  is the proton valence,  $F$  is the Faraday constant,  $\Delta V$  is the transmembrane voltage, and  $\Delta S_o^\ddagger$  and  $\Delta H_o^\ddagger$  are the entropy and enthalpy of activation, respectively. To evaluate  $\Delta S_o^\ddagger$  and  $\Delta H_o^\ddagger$  at a 0 mV, both sides of Eq. 2 are multiplied by the elementary charge ( $e$ ), and following differentiation with respect to voltage at  $V = 0$  (note that proton current  $I_H = ek_H$ ):

$$\left(\frac{dI_H}{dV}\right)_{V=0} = \chi \left(\frac{ekT}{h}\right) \exp\left(\frac{\Delta S_o^\ddagger}{R}\right) \exp\left(\frac{-\Delta H_o^\ddagger}{RT}\right) \left(\frac{zF}{RT}\right) \quad (3)$$

Two other useful thermodynamic relationships are

$$E_a = \Delta H_o^\ddagger + RT \quad (4)$$

$$\Delta G_o^\ddagger = \Delta H_o^\ddagger - T\Delta S_o^\ddagger, \quad (5)$$

where  $\Delta G_o^\ddagger$  is the free energy of activation. These energies relate to the transition to the activated state of the rate-limiting step for proton transfer in gA channels. As such,  $\Delta H_o^\ddagger$  is closely related to the energy barrier height of the activated-state complex, and the entropy of activation ( $\Delta S_o^\ddagger$ ) relates to the ratio between the number of available configurations of the activated complex to those of the reactants (Guerasimov et al., 1974; Berry et al., 2000).

The various energies of activation (free, enthalpy, and entropy) for the activated complex were calculated using Eqs. 1–5.  $E_a$  was determined

experimentally from the slope of Eq. 1 above, and  $(dI/dV)_{V=0}$  was calculated at 298 K according to

$$\left(\frac{dI_H}{dV}\right)_{V=0} = \left(\frac{g_H}{[H]}\right), \quad (6)$$

where  $[H] = [H]_{\text{bulk}} = 1$  M for GMO bilayers. Notice that  $k_H$  in Eq. 2 has the dimension of a second-order rate constant  $(\text{s} \times \text{M})^{-1}$  whereas the right side of Eq. 2 has apparently the dimension of  $\text{s}^{-1}$  (Jordan, 1979; Norris, 1971).

Because DiPhPC bilayers are positively charged in our experimental conditions,  $[H]$  at the membrane-channel/solution interface is not  $[H]_{\text{bulk}}$  (1 M in this work) as with a GMO bilayer but a considerably smaller concentration ( $\sim 58$  mM at the channel-bilayer/solution interface (see Godoy and Cukierman, 2001, for calculations). Therefore, the fact that  $g_H$  in various gA channels in GMO is larger than in DiPhPC bilayers at 1 M  $[H]_{\text{bulk}}$  must take into consideration that gA channels in these two bilayers effectively see different concentrations of protons at the channel's mouths. Once this effect is factored in,  $g_H$  of gA channels in DiPhPC bilayers become considerably larger than in GMO membranes (see Fig. 6 in Godoy and Cukierman, 2001). Consequently, for DiPhPC bilayers,  $[H]$  in Eq. 5 is 0.058 M.

### Some additional remarks

The thermodynamic treatment of our data is general and independent of a specific molecular model. Some possibilities for the rate-limiting step of proton transfer in gA channels include 1) the reorientation of water molecules inside the pore of the channels as in a typical Grothuss mechanism (see Discussion) and/or 2) entry/exit of protons from the channel (Phillips et al., 1999). It is assumed that the generality of our treatment extends to these processes. Also in this regard, it should be noted that the transmission coefficient for proton diffusion or water reorientation is not known.

Implicit in Eq. 3 is that there is no volume change upon the transition to the activated state; i.e., the change in the internal energy ( $\Delta U_0^\ddagger$ ) of the system is given essentially by  $\Delta H_0^\ddagger$  (Guerasimov et al., 1974).

The kinetic theory of the activated state (Eq. 2) does not predict a linear relationship in Arrhenius plots. Not only is  $T$  present in the factor  $(kT/h)$ , but the activation entropy itself is usually a function of  $T$  (Berry et al., 2000). Apparently, the enthalpic component term in Eq. 2  $[\exp(-\Delta H_0^\ddagger/RT)]$  dominates the temperature dependence of  $k_H$ . It has been argued that deviations from linearity in Arrhenius plots are, in general, too small to be detected experimentally (Guerasimov et al., 1974).

## RESULTS

Fig. 1 shows representative single-channel recordings of native gA channels in DiPhPC bilayers at a transmembrane voltage of 50 mV and at three different temperatures. As the bath temperature increased,  $g_H$  increased from 650 pS (top recording) to 825 pS and 1138 pS (middle and bottom recordings, respectively). The single-channel current recordings shown in this as well as in the other figures of this paper were from distinct ion channels in various bilayers (see Materials and Methods). Proton currents in response to voltage clamp ramps are shown in Fig. 2 for the SS channel at various temperatures (see legend). The current-voltage relationships within that voltage range are ohmic. It should be remarked, however, that in 1 M HCl and for voltages larger than  $\sim 100$  mV, the proton currents are supralinear in both GMO and in DiPhPC bilayers (results not shown). The

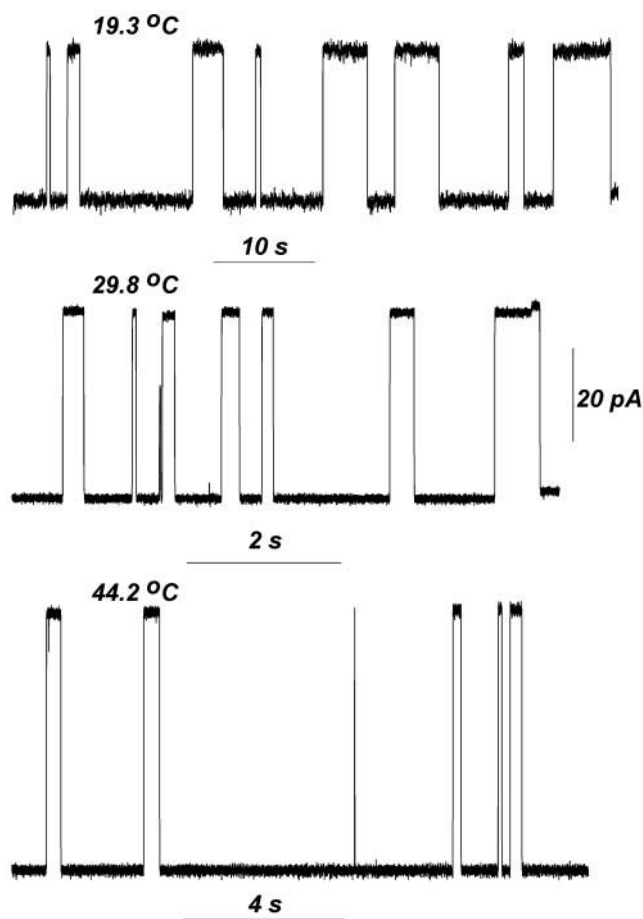


FIGURE 1 Representative single-channel recordings of native gA in DiPhPC bilayers at various temperatures in 1 M HCl solutions. Upward deflections of the current trace are channel openings. The vertical calibration bar applies to all recordings. The transmembrane voltage was 50 mV. Single-channel recordings were originally filtered at 1 kHz and digitized at 5 kHz.

RR channel has a qualitatively similar temperature dependence as the SS channel, showing a monotonic increase in  $g_H$  with temperature and displaying supralinearity in the current-voltage relationships for voltages above  $\sim 100$  mV (results not shown) for both types of bilayers. Although the dependence of  $g_H$  on temperature is qualitatively similar for the various gA channels, there are meaningful quantitative differences.

Fig. 3 shows Arrhenius plots ( $\ln(g_H)$  versus  $1/T$ ) for native gA channels and for the diastereoisomers SS and RR of the dioxolane-linked gA channels. The open and filled circles in all graphs were obtained in GMO and in DiPhPC bilayers, respectively. Linear regression lines and correlation coefficients are also shown for the various plots (see legend). Within the temperature range of 5–45°C, the single-channel proton conductances in gA are consistently larger in GMO than in DiPhPC bilayers (Fig. 3, graph gA). This result is in disagreement with measurements by Phil-

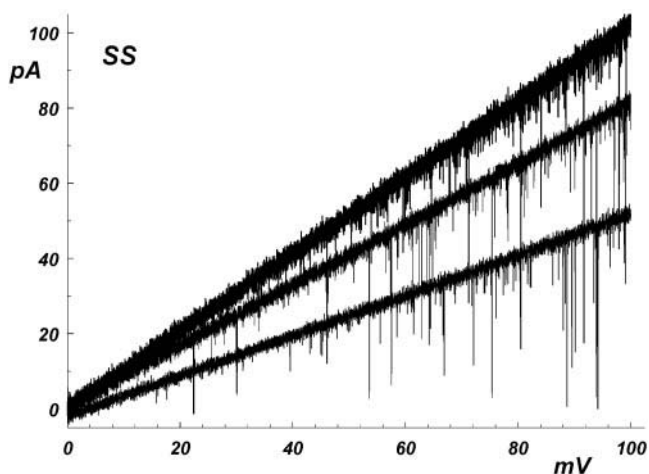


FIGURE 2 Current-voltage relationships in the SS diastereoisomer of the dioxolane-linked gA channel at various temperatures in DiPhPC bilayers. Temperatures and single-channel conductances were (from top to bottom): 44.0°C and 1034 pS, 24.5°C and 798 pS, and 16.0°C and 540 pS. Currents were low-pass Bessel-filtered at 2 kHz and digitized at 8 kHz.

lips et al. (1999) who worked in different experimental conditions (GMO/hexadecane and 0.1 M HCl concentrations). The Arrhenius plots for gA show that although  $g_H$  is larger in GMO than in DiPhPC bilayers, the slopes of the temperature dependencies in different bilayers are basically the same. The activation energies for proton transfer in gA in different bilayers as calculated by regression analyses using Eq. 1 are (mean  $\pm$  SEM)  $15.59 \pm 0.63$  kJ/mol ( $3.73 \pm 0.15$  kcal/mol) for GMO and  $15.34 \pm 0.96$  kJ/mol ( $3.67 \pm 0.23$  kcal/mol) for DiPhPC bilayers. The two gA plots in Fig. 3 have no meaningful signs of departure from linearity.

A different experimental result was reported by Urry et al. (1984) for the temperature dependence of  $g_K$  within a temperature range similar to that shown in Fig. 3. These authors have shown that native gA channels reconstituted in DiPhPC/decane bilayers and in 1 M KCl, have a break (at a temperature of  $\sim 27^\circ\text{C}$ ) in the Arrhenius plot for  $g_K$ . This break defined two distinct activation energies for  $\text{K}^+$  permeation in the gA channel (Fig. 3 in Urry et al., 1984): a low one at high temperatures ( $>27^\circ\text{C}$ ,  $\sim 17$  kJ/mol or 4.06 kcal/mol) and a higher one at low temperatures ( $<27^\circ\text{C}$ ,  $\sim 25$  kJ/mol or 5.98 kcal/mol). In view of the significant implications for the break in linearity of Arrhenius plots for  $g_K$  (Urry et al., 1984, Fig. 3) but not for  $g_H$  in native gA channels (Fig. 3, gA), we have revisited the temperature dependence of  $g_K$  in DiPhPC/decane bilayers in 1 M KCl. Single-channel recordings of gA in 1 M KCl solutions are shown in Fig. 4 at various temperatures (transmembrane potential was 100 mV). The  $g_K$  values were 12.2 pS (at  $9.9^\circ\text{C}$ ), 22.7 pS (at  $24.3^\circ\text{C}$ ), 27.1 pS (at  $29.7^\circ\text{C}$ ), and 38.4 pS (at  $37.4^\circ\text{C}$ ). In Fig. 5, the temperature dependence of  $g_K$  is plotted. Our own experimental measurements of  $g_K$  at

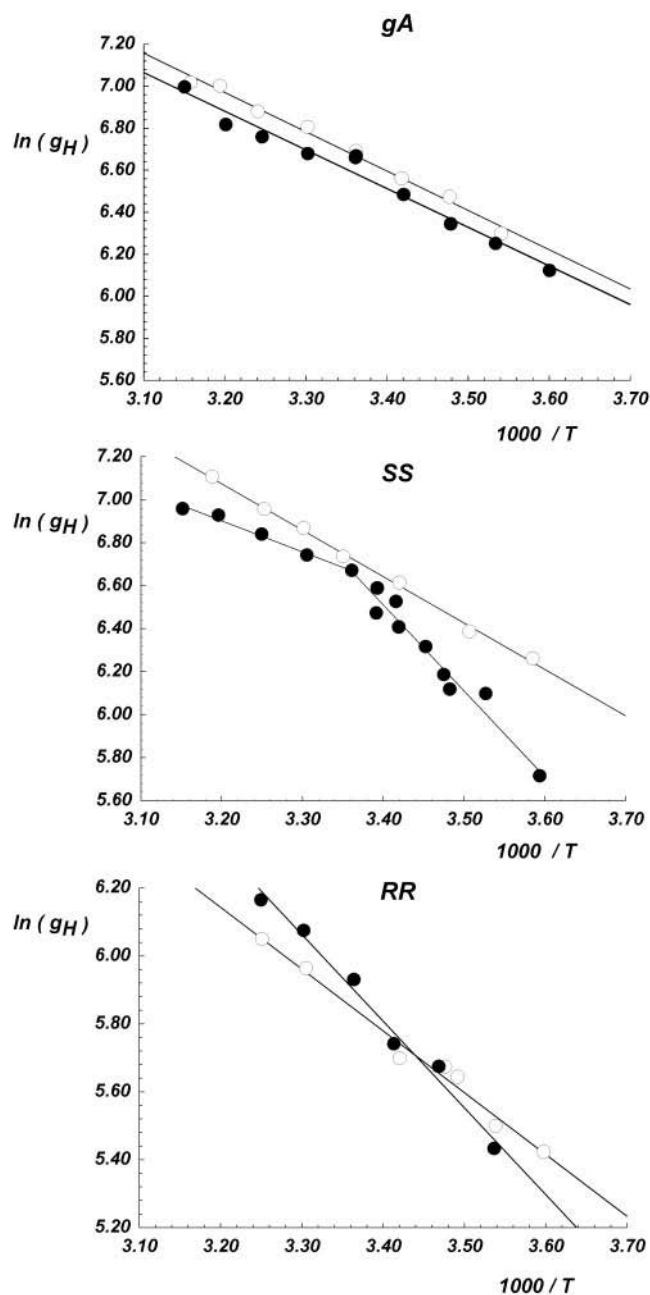


FIGURE 3 Temperature dependencies of  $g_H$  for native gA, SS, and RR dioxolane-linked gA dimers:  $\circ$ , measurements in GMO bilayers;  $\bullet$ , in DiPhPC bilayers. The regression lines are as follows ( $x$  is  $[\ln(1000/K)]$ ): for gA,  $-1.872x + 12.961$  ( $r = 0.990$ ,  $\circ$ ) and  $-1.842x + 12.776$  ( $r = 0.970$ ,  $\bullet$ ); for the SS channel,  $-2.162x + 13.993$  ( $r = 0.997$ ,  $\circ$ ),  $-1.443x + 11.519$  ( $r = 0.988$ ,  $\bullet$  for  $T > \sim 293$  K), and  $-4.000x + 20.108$  ( $r = 0.972$ ,  $\bullet$  for  $T < \sim 293$  K) and for the RR channel,  $-1.821x + 11.969$  ( $r = 0.984$ ,  $\circ$ ) and  $-2.554x + 14.490$  ( $r = 0.985$ ,  $\bullet$ ). Errors of linear fittings are mentioned in text and Table 3.

various temperatures were well fit by a straight line. The activation energy for  $\text{K}^+$  permeation in native gA channels is  $30.04 \pm 0.41$  kJ/mol ( $7.18 \pm 0.10$  kcal/mol), which is almost twice as large as for  $\text{H}^+$  (see Discussion). Thus, our



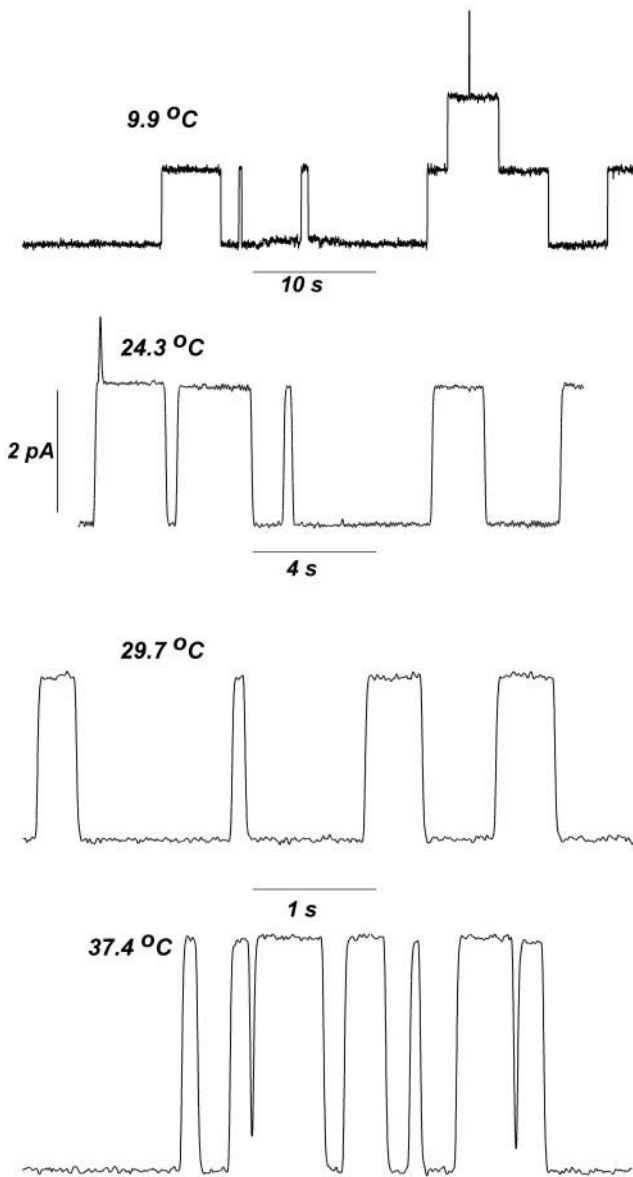


FIGURE 4 Recordings of single  $g_A$  channels in DiPhPC bilayers in 1 M KCl at various temperatures. The membrane voltage was 100 mV. Upward deflections are single-channel openings. Channel currents were originally low-pass Bessel-filtered at 100 Hz and for illustration purposes digitally filtered at 20 Hz. The vertical calibration bar applies to all recordings. The 1-ms calibration bar applies to the recordings at the bottom of the figure. To keep all panels in this figure at the same scale and the figure within a reasonable size, additional and overlapping openings of  $g_A$  channels in the two upper panels are not completely resolved.

own experimental observations suggest that there are no significant departures from linearity in Arrhenius plots for either  $g_H$  or  $g_K$  in the temperature range of 5–45°C in native  $g_A$  channels and in DiPhPC/decane bilayers.

As with native  $g_A$  channels, the SS dioxolane-linked dimer also has a linear Arrhenius plot in GMO membranes. Notice that  $g_H$  values in GMO are consistently larger than in

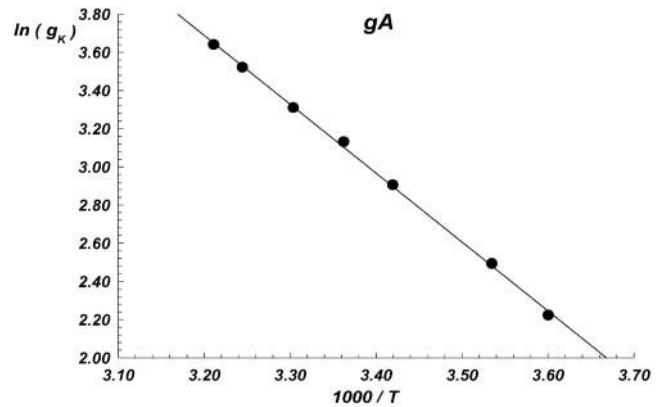


FIGURE 5 Arrhenius plot of  $g_K$  in 1 M KCl in DiPhPC bilayers. The regression line is  $-3.608x + 15.236$  ( $r = 0.999$ ).

DiPhPC at all temperatures (Fig. 3, SS). This observation is in qualitative agreement with  $g_A$  data. However, the activation energy for proton transfer in the SS in GMO membranes is  $18.00 \pm 0.43$  kJ/mol ( $4.30 \pm 0.10$  kcal/mol), which is larger than for native  $g_A$ . The temperature dependence of  $\ln(g_H)$  for the SS in DiPhPC membrane has a break at  $\sim 20^\circ\text{C}$ . This break defines two lines with distinct slopes corresponding to activation energies of  $12.01 \pm 0.48$  kJ/mol ( $2.87 \pm 0.11$  kcal/mol) for temperatures  $>20^\circ\text{C}$  and of  $33.30 \pm 2.22$  kJ/mol ( $7.96 \pm 0.53$  kcal/mol) for temperatures  $<20^\circ\text{C}$ . This break in the Arrhenius plot for the SS in DiPhPC bilayers prompted us to address the generality of this phenomenon for other permeating cations. Consequently, the temperature dependence of  $g_K$  for the SS channel was also evaluated in DiPhPC bilayers. Fig. 6 shows representative recordings of various SS channels at distinct temperatures: at  $5^\circ\text{C}$  (top recording),  $g_K$  is  $\sim 8$  pS, which increases to 12.8 pS ( $24.3^\circ\text{C}$ , middle panel) and 20 pS ( $30.0^\circ\text{C}$ , bottom recording). Because the SS channel under these experimental conditions does not show frequent closures (at a filter frequency of 100 Hz),  $g_K$  values were usually measured at the time of incorporation of the channel in the bilayer. Fig. 7 shows that the Arrhenius plot for  $g_K$  does not have a break in linearity as demonstrated in Fig. 3 for the SS with permeating protons. The corresponding activation energy for  $\text{K}^+$  permeation in the SS channel in DiPhPC bilayers is  $18.02 \pm 1.40$  kJ/mol ( $4.31 \pm 0.33$  kcal/mol). Interestingly, this is about the same as for proton transfer in the SS channel in GMO bilayers. Our preliminary conclusion at this point is that the break in linearity of Arrhenius plots for the SS channel in DiPhPC bilayers appears to be limited to experimental conditions in which protons are the permeating cations.

The temperature dependency of  $g_H$  for the RR dimer is quite different from the SS (Fig. 3, RR). The previous observations that  $g_H$  values are considerably smaller in the RR than in the SS or  $g_A$  (at room temperature, see Armstrong et al., 2001; Cukierman, 2000; Quigley et al., 1999)

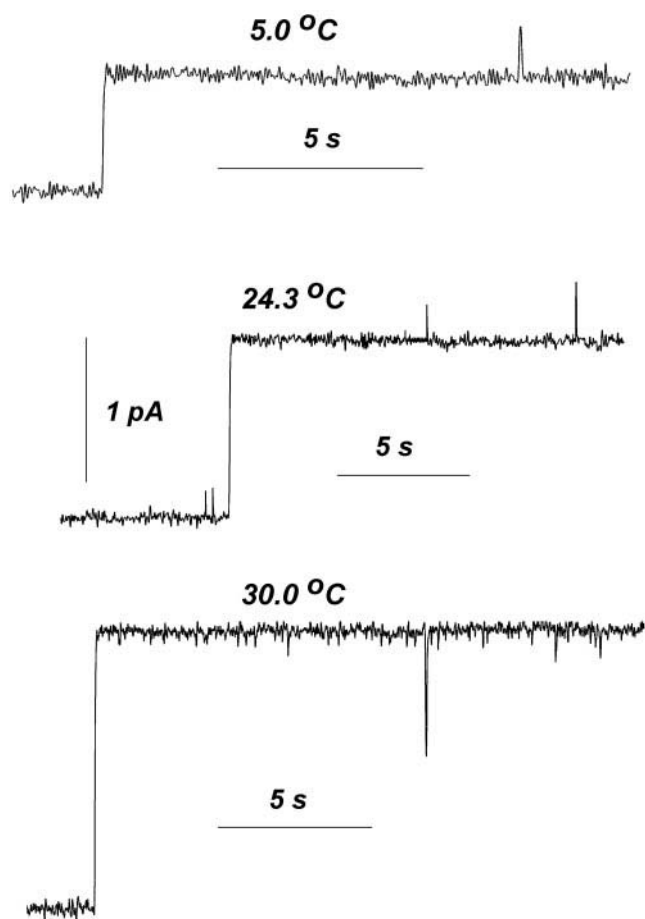


FIGURE 6 Single SS channels in DiPhPC bilayers in 1 M KCl at several temperatures. The membrane voltage was 100 mV. The same vertical calibration bar applies to all recordings. Single-channel recordings were low-pass Bessel filtered at 100 Hz and for the purpose of this illustration were digitally low-pass filtered at 20 Hz. See text for description.

are now extended to a wider temperature range (Fig. 8). The activation energy for proton transfer in the RR in GMO ( $15.16 \pm 0.86$  kJ/mol or  $3.62 \pm 0.21$  kcal/mol) is considerably lower than in the SS and about the same as gA in GMO. In DiPhPC bilayers, however, the activation energy for proton transfer in the RR ( $21.27 \pm 1.30$  kJ/mol or  $5.08 \pm 0.31$  kcal/mol) is considerably larger than in GMO bilayers. In contrast to native gA channels, the activation energies for proton transfer in both the SS and RR channels are strongly influenced quantitatively and qualitatively by the lipid environment.

## DISCUSSION

The novel experimental results in this study relate to the measurements of activation energies of proton transfer in native and dioxolane-linked gA channels in distinct lipid bilayers. We have shown that in general, and within the temperature range of 5–45°C, there is a typical Arrhenius

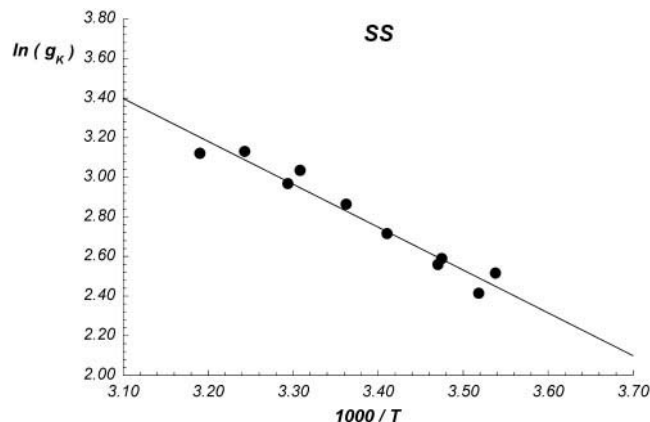


FIGURE 7 Arrhenius plot of  $g_K$  in the dioxolane-linked SS dimer in DiPhPC bilayers. The regression line is  $-2.305x + 10.108$  ( $r = 0.958$ ).

relationship for the various gA channels studied in this work. The exception is the SS dioxolane-linked gA channel reconstituted in DiPhPC bilayers whose data could not be adequately fit by a single straight line. The rest of the discussion is divided in three parts. First and second, the activation energies for ion diffusion in water and in biological channels will be addressed. Third, the activation thermodynamics of proton transfer in gA channels will be discussed.

## Activation energies for ionic diffusion in water

The activation energy for proton transfer in water is significantly smaller than for the diffusion of any other ion, or for the self-diffusion of water. The  $E_a$  for proton transfer in bulk water is 11.29 kJ/mol (Table 1). The  $E_a$  values for the aqueous diffusion of  $\text{Ca}^{2+}$ ,  $\text{K}^+$ , for example, and for water self-diffusion are 14.62, 16.74, and 18.41 kJ/mol, respectively (Table 2). These results together with the well known fact that proton mobility in water cannot be predicted (even approximately as with other ions) by classical hydrodynamic relationships (Stokes's law) suggest that proton transfer in water has a unique character. Historically, proton transfer in water has been rationalized by a hop and turn mechanism (also known as the Grotthuss's mechanism). Once a proton approaches the O of a water molecule, it eventually forms a new OH covalent bond, releasing one  $\text{H}^+$  from one of the two original OH covalent bonds in that water molecule. The released proton is then shared between two adjacent water molecules ( $(\text{H}_5\text{O})^+$ ). This hopping step propagates along the H-bonded chain of water molecules causing the proton to be transferred across the entire water chain. As the proton hops, the orientation of the dipole moments of all water molecules attain a configuration that is approximately 180° opposite to that found in the beginning of the process (see for example Fig. 1 in Godoy and Cukierman, 2001). For another proton to be transferred in the

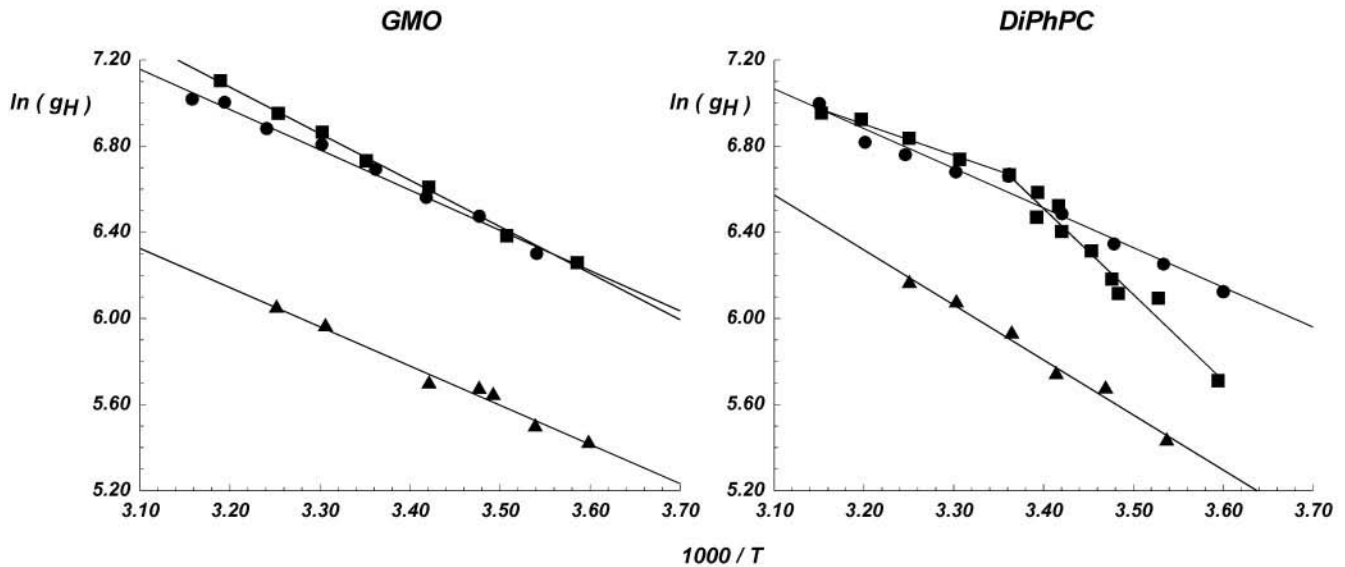


FIGURE 8 The data points in Fig. 3 were regrouped in this figure with the aim of illustrating in the same lipid bilayer the single-channel proton conductances of various gA channels. The expressions for the regression lines are the same as mentioned in Fig. 3. ●, ■, and ▲,  $g_H$  in native gA, SS, and RR channels, respectively.

same direction along the water chain, it is necessary for the water molecules to flip back to their original configuration (turn step, Bernal and Fowler, 1933; Conway et al., 1956; Nagle and Tristram-Nagle, 1983; Pomès and Roux, 1996, 1998). The rate-limiting step for proton transfer in aqueous solution has been attributed to the turn step (reorientation of water molecules, Bernal and Fowler, 1933; Conway et al., 1956).

The contrasting behavior between the  $E_a$  for water rotation and proton mobility over a wide range of temperatures was one of the factors that allowed Agmon (1995, 1996) to propose that water rotation is not the rate-limiting step in proton transfer. Water molecules in bulk are usually tetrahedrally coordinated (each water donates to and accepts two

H-bonds from adjacent water molecules). For water rotation to occur, at least three H-bonds must first be broken. It has been estimated that the total energy of these H-bonds is  $\sim 57$  kJ/mol, which is  $\sim 5$ -fold the  $E_a$  for proton transfer in water ( $\sim 11$  kJ/mol, Table 1). On the other hand, an  $E_a$  of  $\sim 11$  kJ/mol is approximately the energy of one H-bond between the first and second solvation shells of a  $(H_3O)^+$  cation (Agmon, 1996). It has been proposed that the disruption of this H-bond limits the transfer of protons in water (Agmon, 1996). This idea has recently received significant support from computational studies of an excess proton in bulk water (Day et al., 2000; Schmitt and Voth, 1999).

Because gramicidin channels are water-filled pores containing a one-dimensional chain of water molecules (Levitt, 1984; Finkelstein, 1987; Pomès and Roux, 1996), it is of interest to examine what happens with proton transfer in such systems. Proton transfer in an isolated H-bonded chain of nine polarizable (PM6 model) water molecules was studied with classical molecular dynamics simulations in the presence or absence of an excess proton (Pomès and Roux, 1998; Pomès, 1999). Proton hopping is essentially activationless whereas the free energy for reorientating nine water molecules is  $\sim 32$  kJ/mol. This figure is  $\sim 3$ -fold larger than in bulk water).

In conclusion, there are significant qualitative and quantitative differences between the rate-limiting steps for proton transfer in bulk water and in computational studies with one-dimensional water wires. Although in the former (water has a coordination number of 3–4), the energy for disrupting a H-bond between waters in the first and second solvation shells of  $(H_3O)^+$  agrees with the  $E_a$  for proton transfer

TABLE 1 Activation energies for proton transfer

	$E_a$ (kJ/mol)	
	GMO	DiPhPC
gA	15.59	15.34
SS	18.00	12.01 <sup>HT</sup> , 33.30 <sup>LT</sup>
RR	15.16	21.27
gA*		20
ACM <sup>†</sup>		75 <sup>HT</sup> , 113 <sup>LT</sup>
0.1 mM HCl <sup>‡</sup>		11.29
1 M HCl <sup>‡</sup>		10.79

HT, high-temperature range ( $>20^\circ\text{C}$ ); LT, low-temperature range ( $<20^\circ\text{C}$ , this work).

\*Measured in GMO/cholesterol bilayers (Akeson and Deamer, 1991).

<sup>†</sup>Macroscopic proton currents measured across macropatches of alveolar cell membranes (DeCoursey and Cherny, 1998). LT and HT were calculated for temperatures lower or higher than  $20^\circ\text{C}$ , respectively.

<sup>‡</sup>Weast, 1990.

**TABLE 2** Activation energies for several nonproton conductivities

	$E_a$
SR $\text{Ca}^{2+}$ -release channel*	26
SR $\text{K}^+$ -selective channel <sup>†</sup>	20–50
$\text{Ca}^{2+}$ -activated $\text{K}^+$ channel <sup>‡</sup>	30
Voltage dependent $\text{Na}^+$ channels <sup>§</sup>	28
$g_{\text{Na}}$ in gA	(36–44) <sup>¶</sup> , 21 <sup>  </sup> , (19 and 31)**
$g_{\text{K}}$ in gA	(17 <sup>HT</sup> 25 <sup>LT</sup> ) <sup>††</sup> , 22 <sup>  </sup>
$g_{\text{K}}$ in gA <sup>‡‡</sup>	30.04
$g_{\text{K}}$ in SS <sup>‡‡</sup>	18.02
$\text{K}^+$ <sup>§§</sup>	14.62
$\text{Ca}^{2+}$ <sup>§§</sup>	16.74
$\text{H}_2\text{O}$ <sup>¶¶</sup>	18.41

DeCoursey and Cherny (1998) should be consulted for a more comprehensive compilation of results of various other channels.

\*SR, sarcoplasmic reticulum;  $\text{Ca}^{2+}$  channels in lipid bilayers (Sitsapesan et al., 1991).

<sup>†</sup>Measurements performed in lipid bilayers with alkaline metals (Miller, 1988).

<sup>‡</sup>Patch-clamp measurements (Grygorczyk, 1987).

<sup>§</sup>Patch clamp measurements (Milburn et al., 1995).

<sup>¶</sup><sup>23</sup>Na-NMR measurements in membrane vesicles with native and phenylalanine analogs of gA (Hinton et al., 1993).

<sup>||</sup>Hladky and Haydon, 1974 (GMO bilayers).

\*\*19 and 31 kJ/mol in GMO and in dioleoyllecithin bilayers, respectively (Bamberg and Lauger, 1974).

<sup>††</sup>Measurements done in DiPhPC bilayers (Urry et al., 1984). A break in the Arrhenius plot around 300 K was shown in that study. HT and LT were estimated by us for temperatures higher or lower than 27°C, respectively.

<sup>‡‡</sup>This study (DiPhPC bilayers).

<sup>§§</sup>Activation energies of  $\text{K}^+$  and  $\text{Ca}^{2+}$  conductivities in dilute aqueous solutions (limiting conductivities, Robinson and Stokes, 1959).

<sup>¶¶</sup>Temperature dependence of the self-diffusion coefficient of water (Eisenberg and Kauzman, 1969).

in bulk water, in a one-dimensional apolar water wire (water has a coordination number of 2–3), the reorientation of the total dipole moment of a one-dimensional water chain seems to be the rate-limiting step of proton transfer.

### Activation energies for ionic permeation in biological channels

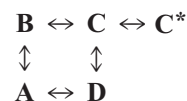
In Tables 1 and 2, the activation energies for proton and some nonproton permeation in various ion channels are shown. In compiling these data, studies of reconstituted ion channels in simple well-defined lipid bilayer systems were

avored. In general, and in qualitative agreement with ionic diffusion in water, the activation energies for proton transfer in gA channels are lower than with nonproton permeation in gA or in other ion channels. Although typical activation energies for protons are under 20 kJ/mol, activation energies for permeation of alkaline cations and  $\text{Ca}^{2+}$  are in the range of 20–50 kJ/mol. DeCoursey and Cherny (1998) measured the  $E_a$  for macroscopic proton currents in macropatches of cell membranes from alveolar epithelia. Their measured  $E_a$  (see Table 1) for protons is significantly larger than in various gA channels reported here, and by Akesson and Deamer (1991). The basic mechanism by which protons permeate those epithelial channels is not known, and one possibility is that proton transfer in those channels may not be mediated by a typical water wire mechanism discussed above.

### Activation energies for protons in gA channels

#### GMO bilayers

To visualize the effects of temperature on various gA channels in the same type of lipid bilayer, data in Fig. 3 were replotted in Fig. 8. The left and right graphs of this figure show Arrhenius plots for the various gA channels in GMO and DiPhPC bilayers, respectively. Even though  $g_{\text{H}}$  in the RR channel is considerably smaller than in the SS (or native gA channels) over the entire temperature range of this study, the activation energy for proton transfer in the RR channel in GMO membranes is smaller than for the SS or native gA channels (Table 1). The activation enthalpy (which parallels  $E_a$ ) is smaller in the RR than in native gA or SS channels (Table 3). Thus, the smaller  $g_{\text{H}}$  in the RR channel can be explained by a considerably larger activation entropy (more negative, see Eq. 2 and Table 3) in the RR than in the SS or native gA channels. It seems that it is this entropy that causes a larger  $\Delta G_o^\ddagger$  for the RR in relation to the other gA channels (Table 3). A qualitative model that could account for differences in activation energies between the RR and the SS or native gA channels is, as an example,

**TABLE 3** Activation enthalpies, entropies, and Gibbs free energies for proton currents in various gA channels

	$\Delta H_o^\ddagger$ (kJ/mol)		$\Delta S_o^\ddagger$ (J/K · mol)		$\Delta G_o^\ddagger$ (kJ/mol)	
	GMO	DiPhPC	GMO	DiPhPC	GMO	DiPhPC
gA	13.11 ± 0.63	12.86 ± 0.96	-45.61 ± 2.17	-23.05 ± 2.17	26.70 ± 0.02	19.73 ± 0.02
SS	15.52 ± 0.43	9.54 ± 0.48	-37.15 ± 1.60	-34.12 ± 1.60	26.59 ± 0.06	19.70 ± 0.07
RR	12.68 ± 0.86	18.79 ± 1.30	-54.24 ± 3.37	-9.21 ± 3.37	28.85 ± 0.14	21.53 ± 0.06

The figures shown in this Table for the SS channel in DiPhPC bilayers are those corresponding to the low-activation-energy region of the Arrhenius plot (temperatures >20°C). Values are expressed as mean ± SEM. Standard errors were calculated from the SEMs of Arrhenius plots (see Fig. 3 and text).



In the kinetic scheme above, A to D are four conformational states of the RR channel in which proton transfer does not occur. Ultimately, these states define conformations of the water wire inside the RR channel that cannot transfer protons via a Grotthuss mechanism. This would have the effect of increasing the entropy of proton transfer in the RR in relation to other gA channels. On the other hand, C\* is a conformational state in which protons are transferred along the water wire (hop and turn steps) and can be reached only from the C state. We postulate that the smaller  $g_H$  in the RR channels is accounted for by a larger number of A· · · D states in the RR than in native gA or SS channels, and not by a larger activation enthalpy. In fact, our molecular dynamic models with the dioxolane-linked gA channels (Yu, Cukierman, and Pomès, manuscript in preparation) show that the dihedrals immediately adjacent to the RR dioxolane linker have stable configuration states that are not shared by the SS dioxolane in gA-linked channels. Some of these conformations (A· · · D) could change the H-bonding pattern between channel and channel waters in such a way as to compromise the Grotthuss mechanism in the pore.

The  $\Delta G_o^\ddagger$  values for proton transfer in the SS and gA channels are nearly the same in GMO (as well as in DiPhPC, see below) bilayers (Table 3). The activation entropies and enthalpies however, are not. The  $\Delta S_o^\ddagger$  is more negative in the native gA than in the SS channel. In native gA channels, we would expect several conformational states that result from the dynamics between two free gA monomers. On the other hand, the SS dioxolane would constrain the dynamics between the two gA molecules. This could have the effect of reducing the number of possible conformational states that do not transfer protons along the water wire in the SS in relation to native gA channels. In fact, the original idea for developing the dioxolane-linked gA dimers was that the SS dioxolane provides a continuous and constrained transition between the right-handed  $\beta$ -helices of two gA molecules (Stankovic et al., 1989).

On the other hand,  $\Delta H_o^\ddagger$  is larger for the SS than for native gA channels. The presence of two extra oxygens in the dioxolane in middle of the SS channel is likely to enhance the negative electric field in the middle of the pore, in relation to native gA channel. This could stabilize the water molecules in the middle of the channel and hamper the turn step in a Grotthuss mechanism, thus increasing  $\Delta H_o^\ddagger$ .

In GMO bilayers and at 298 K, the enthalpic components [ $\exp(-\Delta H_o^\ddagger/RT)$ ] are  $\sim 5.06 \times 10^{-3}$  (gA),  $1.91 \times 10^{-3}$  (SS), and  $6.01 \times 10^{-3}$  (RR). The entropic components [ $\exp(\Delta S_o^\ddagger/R)$ ] are  $4.14 \times 10^{-3}$  (gA),  $1.15 \times 10^{-2}$  (SS), and  $1.47 \times 10^{-3}$  (RR). For native gA channels, the contributions of the enthalpic and entropic components to proton transfer (Eq. 2) are about the same. For the SS channel, the enthalpy of proton transfer activation is more rate limiting than the entropic component. The entropic component for proton transfer activation in the RR channel is more important than the activation enthalpy.

## DiPhPC bilayers

Since the beginning of our studies with the SS and RR dioxolane-linked dimers, it became clear that the single-channel properties of these channels were significantly modulated by the lipid environment (Cukierman, 1999; Cukierman et al., 1997). These previous observations are now extended to a wide range of temperatures.

In DiPhPC bilayers, the SS channel does not show a typical Arrhenius behavior. This point was thoroughly investigated in this study, and we are convinced that there is a clear and significant difference between the activation energies in high ( $>20^\circ\text{C}$ , 13.51 kJ/mol) and low ( $<20^\circ\text{C}$ , 33.30 kJ/mol) temperature ranges. These observations were also confirmed with the conduction of deuterons in the SS channel (Chernyshev and Cukierman, manuscript in preparation). Table 3 presents the results of calculations performed at 298 K, and only energies corresponding to the high temperature range of the SS in DiPhPC bilayers are shown. The break in linearity is not likely to be related to phase transitions in DiPhPC/decane bilayers because the RR and gA channels do not have it. Breaks in linearity in Arrhenius plots are relatively common. In particular, similar phenomena have been noticed by DeCoursey and Cherny (1998) for proton currents in alveolar epithelial cells and by Miller (1988) for the sarcoplasmic reticulum  $\text{K}^+$  channel. It is likely that the SS channel in DiPhPC can adopt two stable and distinct conformations in the low and high ranges of temperatures. Notice that in the low range of temperatures, the proton activation energy is comparable to that measured with alkaline metals in gA and in other channels (Table 2). This prompted us to measure the kinetic isotope effect for proton transfer in different temperatures in the SS in DiPhPC bilayers. Our preliminary results in 1 M DCl show that the ratio  $g_H/g_D$  is  $\sim 1.3$  at temperatures corresponding to the different  $E_a$  values. This kinetic isotope effect appears to be more consistent with a Grotthuss mechanism than with the hydrodynamic flow of  $(\text{H}_3\text{O})^+$  for which a considerably smaller kinetic isotope effect is expected (see for example, Conway et al., 1956).

This break in linearity is not shared by Arrhenius plots of  $g_K$  (Fig. 7), suggesting that it is specific to proton transfer. Whereas more experimental work is necessary to buttress this preliminary conclusion, it appears that the Grotthuss mechanism is far more sensitive to the conformational change occurring with the SS in DiPhPC at different temperatures than the hydrodynamic flow of water and monovalent cations.

In DiPhPC bilayers, gA channels have a larger  $g_H$  than in GMO bilayers. Evidently, this is a consequence of a reduced  $\Delta G_o^\ddagger$  for proton transfer in DiPhPC bilayers (Table 3). The predominant factor underlying this reduced  $\Delta G_o^\ddagger$  in native gA and in the dioxolane-linked RR channel is a decrease in the entropy. The entropic component [ $\exp(\Delta S_o^\ddagger/R)$ ] for gA channels increases from  $4.14 \times 10^{-3}$  (GMO bilayers) to

$6.25 \times 10^{-2}$  (DiPhPC bilayers), and from  $1.47 \times 10^{-3}$  (GMO) to  $3.30 \times 10^{-1}$  (DiPhPC) for the RR channel. In the SS channel, the entropic component is attenuated by a relatively smaller amount in DiPhPC bilayers ( $1.15 \times 10^{-2}$  in GMO, and  $1.65 \times 10^{-2}$  in DiPhPC). GMO has one oleic acid chain whereas DiPhPC has two methyl-branched fatty acid chains. It is possible that the fatty acid chains of DiPhPC have a larger stabilizing effect on the side residues of gA channels than in GMO bilayers. It also seems likely that the viscosity of DiPhPC bilayers is larger than in GMO bilayers. Both effects would constrain the motion of the side chain residues in gA channels. This could reduce the number of possible conformational states in the RR and native gA channels that would ultimately reflect in a smaller number of possible configurations of the water chain inside the channel, favoring an increase of  $g_H$  in DiPhPC in relation to GMO bilayers.

### Comparison with computational studies

Computational studies by Pomès and Roux (1996) demonstrated that proton hopping inside a chain of H-bonded water molecules (water wire) in native gA channels is an activationless process occurring in the picosecond time scale. By contrast, the reorientation of the water wire (turn step in a Grotthuss mechanism) has a free energy of  $\sim 16$  kJ/mol with PM6 polarizable water models (Schumaker et al., 2000) and  $\sim 9$  kJ/mol with TIP3P water molecules (Pomès and Roux, personal communication). Interestingly, the free energy of the reorientation of a column of PM6 waters is comparable to our measurements and calculations for  $\Delta G_o^\ddagger$  in various gA channels in DiPhPC bilayers (Table 3). Despite a significant progress in our understanding of proton transfer dynamics in gA channels, the computational models are incipient and do not consider several factors that modulate  $H^+$  transfer such as the nature of lipid bilayers (Table 3, see Introduction for references) and the channel-membrane/solution interfaces (Phillips et al., 1999; Godoy et al., 2001). It has been recently proposed (Gowen et al., submitted for publication) that the rate-limiting step for  $H^+$  transfer in gA channels is not the reorientation of water wire but the entry/exit rate of protons in the channel. A detailed discussion of the rate-limiting step for proton transfer in gA channels is clearly beyond the scope of this paper. However, whatever the rate-limiting step may be, the free energy of activation of said process must be in consonance with data presented in this paper.

In summary, in this study we have measured the activation energies for proton transfer in dioxolane-linked gA channels and in native gA channels in two distinct lipid bilayers. The  $E_a$  values for proton transfer in gA channels are significantly larger than in aqueous solutions of 1 M HCl (Table 1), indicating that the rate-limiting step for proton transfer in gA channels is not in the bulk solution but in the channel or membrane-channel/solution interface (Go-

wen et al., 2001; Cukierman, 2000; Godoy and Cukierman, 2001). Overall, these activation energies are generally smaller than nonproton single-channel conductances attesting to the uniqueness of proton transfer in gA channels.  $\Delta G_o^\ddagger$  values for proton transfer in the RR channel are considerably larger than in the SS or native gA channels in different lipid bilayers. Our calculations suggest that, in general, the activation entropy has a significant role in determining  $g_H$  in gA channels in GMO or DiPhPC bilayers. We expect that the measurements presented in this study will be useful for checking the plausibility of models for proton transfer in ion channels or proteins.

We thank Dr. David D. Busath for several insightful discussions on the subject of this paper.

This work was supported by the National Institutes of Health (GM59674).

### REFERENCES

- Agmon, N. 1995. The Grotthuss mechanism. *Chem. Phys. Lett.* 244: 456–462.
- Agmon, N. 1996. Hydrogen bonds, water rotation and proton mobility. *J. Chim. Phys.* 93:1714–1736.
- Akeson, M., and D. W. Deamer. 1991. Proton conductance by the gramicidin water wire: model for proton conductance in the  $F_0F_1$ ATPases? *Biophys. J.* 60:101–109.
- Armstrong, K. M., E. P. Quigley, P. Quigley, D. S. Crumrine, and S. Cukierman. 2001. Covalently linked gramicidin channels: effects of linker hydrophobicity and alkaline metals on different stereoisomers. *Biophys. J.* 80:1810–1818.
- Bernal, J. D., and R. H. Fowler. 1933. A theory of water and ionic solution, with particular reference to hydrogen and hydroxyl ions. *J. Chem. Phys.* 1:515–548.
- Berry, R. S., S. A. Rice, and J. Ross. 2000. *Physical Chemistry*, 2nd ed. Oxford University Press, New York.
- Bamberg, E., and K. Janko. 1977. The action of a carbonyl dimerized gramicidin A on lipid bilayer membranes. *Biochem. Biophys. Acta.* 465:486–499.
- Bamberg, E., and P. Lauger. 1974. Temperature-dependent properties of gramicidin A channels. *Biochem. Biophys. Acta.* 367:127–133.
- Conway, B. E., J. O. M. Bockris, and H. Linton. 1956. Proton conductance and the existence of the  $H_3O^+$  ion. *J. Chem. Phys.* 24:834–852.
- Cukierman, S. 1999. Flying protons in linked gramicidin A channels. *Isr. J. Chem.* 39:419–426.
- Cukierman, S. 2000. Proton mobilities in water and in different stereoisomers of covalently linked gramicidin A channels. *Biophys. J.* 78: 1825–1834.
- Cukierman, S., E. P. Quigley, and D. S. Crumrine. 1997. Proton conduction in gramicidin A and in its dioxolane-linked dimer in different lipid bilayers. *Biophys. J.* 73:2489–2502.
- Day, T. J. F., U. W. Schmitt, and G. A. Voth. 2000. The mechanism of hydrated proton transfer in water. *J. Am. Chem. Soc.* 122:12027–12028.
- DeCoursey, T. E., and V. V. Cherny. 1998. Temperature dependence of voltage-gated  $H^+$  currents in human neutrophils, rat alveolar epithelial cells, and mammalian phagocytes. *J. Gen. Physiol.* 112:503–522.
- Eisenberg, D., and W. Kauzmann. 1969. *The Structure and Properties of Water*. Oxford University Press, New York.
- Finkelstein, A. 1987. *Water Movement through Lipid Bilayers, Pores, and Plasma Membrane: Theory and Reality*. John Wiley, New York.
- Godoy, C. M. G., and S. Cukierman. 2001. Modulation of proton transfer in the water wire of dioxolane-linked gramicidin channels by lipid membranes. *Biophys. J.* 81:1430–1438.

- Grygorczyk R. 1987: Temperature dependence of  $\text{Ca}^{2+}$ -activated  $\text{K}^+$  currents in the membrane of human erythrocytes. *Biochem. Biophys. Acta.* 902:159–168.
- Guerasimov Ya., V. Dreving, E. Eremin, A. Kiselev, V. Lebedev, G. Panchenkov, and A. Shlygin. 1974. Physical Chemistry, Vol. 2. Mir Publishers, Moscow.
- Hinton, J. F., P. L. Easton, D. K. Newkirk, and D. C. Shungu. 1993.  $^{23}\text{Na}$ -NMR study of ion transport across vesicle membranes facilitated by phenylalanine analogs of gramicidin. *Biochim. Biophys. Acta.* 1146: 191–196.
- Hladky, S. B., and D. A. Haydon. 1972. Ion transfer across lipid membranes in the presence of gramicidin A. I. Studies of the unit conductance channel. *Biochem. Biophys. Acta.* 274:294–312.
- Jordan, P. C. 1979. Chemical Kinetics and Transport. Plenum Press, New York.
- Jordan, P. C. 1999. Ion permeation and channel kinetics. *J. Gen. Physiol.* 114:601–603.
- Koeppe, R. E. II, and O. S. Andersen. 1996. Engineering the gramicidin channel. *Annu. Rev. Biophys. Biomol. Struct.* 25:231–258.
- Levitt, D. G. 1984. Kinetics of movement in narrow channels. *Curr. Top. Membr. Transp.* 21:181–197.
- Milburn, T., D. A. Saint, and S. H. Chung. 1995. The temperature dependence of conductance of the sodium channel: implications for mechanism of ion permeation. *Receptors Channels.* 3:201–211.
- Miller, C. 1988. A thermodynamic analysis of monovalent cation permeation through a  $\text{K}^+$ -selective ion channel. *Neuron.* 1:159–164.
- Nagle, J. F., and S. Tristram-Nagle. 1983. Hydrogen bonded chain mechanisms for proton conduction and proton pumping. *J. Membr. Biol.* 74:1–14.
- Norris, A. C. 1971. SI units in physico-chemical calculations. *J. Chem. Ed.* 48:797–800.
- Phillips, L. R., C. D. Cole, R. J. Hendershoot, M. Cotten, T. A. Cross, and D. D. Busath. 1999. Non-contact dipole effects on channel permeation. III. Anomalous proton conductance effects in gramicidin. *Biophys. J.* 77:2492–2501.
- Pomès, R. 1999. Theoretical studies of the Grotthuss mechanism in biological proton wires. *Isr. J. Chem.* 39:387–395.
- Pomès, R., and B. Roux. 1996. Structure and dynamics of a proton wire: a theoretical study of  $\text{H}^+$  translocation along the single-file water chain in the gramicidin A channel. *Biophys. J.* 71:19–39.
- Pomès, R., and B. Roux. 1998. Free energy profiles for  $\text{H}^+$  conduction along hydrogen-bonded chains of water molecules. *Biophys. J.* 75: 33–40.
- Quigley, E. P., D. S. Crumrine, and S. Cukierman. 2000. Gating and permeation in ion channels formed by gramicidin A and its dioxolane-linked dimer in  $\text{Na}^+$  and  $\text{Cs}^+$  solutions. *2000. J. Membr. Biol.* 174: 207–212.
- Quigley, E. P., P. Quigley, D. S. Crumrine, and S. Cukierman. 1999. The conduction of protons in different stereoisomers of dioxolane-linked gramicidin A channels. *Biophys. J.* 77:2479–2491.
- Robinson, R. A., and R. H. Stokes. 1959. Electrolyte Solutions, 2nd ed. Butterworths, London.
- Rudnev, V. S., L. N. Ermishkin, L. A. Fonina, and Y. G. Rovin. 1981. The dependence of the conductance and lifetime of gramicidin channels on the thickness and tension of lipid bilayers. *Biochem. Biophys. Acta.* 642:196–202.
- Schmitt, U. W., and G. A. Voth. 1999. The computer simulation of proton transfer in water. *J. Chem. Phys.* 111:9361–9381.
- Schumaker, M. F., R. Pomès, R., and B. Roux. 2000. A framework model for single proton conductance through gramicidin. *Biophys. J.* 79: 2840–2857.
- Sitsapesan, R., R. A. Montgomery, K. T. MacLeod, and A. J. Williams. 1991. Sheep cardiac sarcoplasmic reticulum calcium-release channels: modifications of conductance and gating by temperature. *J. Physiol.* 434:469–488.
- Stankovic, C. J., S. H. Heinemann, and S. L. Schreiber. 1990. Immobilizing the gate of a tartaric acid-gramicidin A hybrid channel molecule by rational design. *J. Am. Chem. Soc.* 112:3702–3704.
- Stankovic, C. J., S. H. Heinemann, J. M. Delfino, F. J. Sigworth, and S. L. Schreiber. 1989. Transmembrane channels based on tartaric acid-gramicidin A hybrids. *Science.* 244:813–817.
- Urry, D. W. 1971. Gramicidin A transmembrane channel: a proposed  $\text{P}_{(L, D)}$  helix. *Proc. Natl. Acad. Sci. U.S.A.* 68:672–676.
- Urry, D. W., S. Alonso-Romanowski, C. M. Ventakachalam, R. J. Bradley, and R. D. Harris. 1984. Temperature dependence of single channel currents and the peptide libration mechanism for ion transport through the gramicidin A transmembrane channel. *J. Membr. Biol.* 81:205–217.
- Weast, R. C. 1990. Handbook of Physics and Chemistry, 70th ed. CRC Press, Boca Raton, FL.